H-mode Research in NSTX

R. Maingi 1), M.G. Bell 2), R.E. Bell 2), C.E. Bush 1), E.D. Fredrickson 2), D.A. Gates 2), T. Gray 3), D.W. Johnson 2), R. Kaita 2), S.M. Kaye 2), S. Kubota 4), H.W. Kugel 2), C.J. Lasnier 5), B.P. LeBlanc 2), R.J. Maqueda 6), D. Mastrovito 2), J.E. Menard 2), D. Mueller 2), M. Ono 2), F. Paoletti 7), S.J. Paul 2), Y-K.M. Peng 1), A.L. Roquemore 2), S.A. Sabbagh 7), C.H. Skinner 2), V.A. Soukhanovskii 2), D. Stutman 8), E.J. Synakowski 2), T. Tan 9), J.B. Wilgen 1), S.J. Zweben 2)

1) Oak Ridge National Laboratory, Oak Ridge TN, 37831 USA
2) Princeton Plasma Physics Laboratory, PO Box 451, Princeton, NJ, 08543 USA
3) North Carolina State University, Raleigh, NC 27695 USA
4) University of California at Los Angeles, Los Angeles, CA USA
5) Lawrence Livermore National Laboratory, Livermore, CA USA
6) Los Alamos National Laboratory, Los Alamos, NM, 87545 USA
7) Columbia University, New York, NY, USA
8) Johns Hopkins University, Baltimore, MD, USA
9) West-Windsor/Plainsboro High-School North, Plainsboro NJ 08536 USA

Abstract. H-modes are routinely obtained in NSTX and have become a standard operational scenario. L-H transitions triggered by NBI heating have been obtained over a wide parameter range in I_p, B_t, and $\overline{n_e}$ in either lower-single null (LSN) or double-null (DN) diverted discharges. ELMs are observed in both configurations but the characteristics differ between DN and LSN, which also have different triangularity(δ). H-mode duration of 500 msec was obtained in LSN, with total pulse length ~ 1 sec. Preliminary power threshold studies indicate the L-H threshold is between 600 kW and 1.2 MW, depending on target parameters. Gas injector fueling from the center stack (i.e. the high toroidal field side) has enabled routine H-mode access, and comparisons with low-field side (LFS) fueled H-mode discharges show that the LFS fueling delays the L-H transition and alters the pre-transition plasma profiles. Gas puff imaging and reflectometry show that the H-mode edge is usually more quiescent than the L-mode edge. Divertor infrared camera measurements indicate up to 70% of available power flows to the divertor targets in quiescent H-mode discharges.

The National Spherical Torus Experiment (NSTX) is a medium-size low aspect ratio spherical torus[1,2] with both neutral beam and radio-frequency auxiliary heating (R=0.86m, a=0.67m, R/a $\geq$ 1.26, $B_t \leq 0.6$ T, $I_p \leq 1.5$ MA, $P_{NBI} \leq 7$ MW, $P_{RF} \leq 6$ MW). Making a determination of the attractiveness of the spherical torus concept in the areas of high-β stability, confinement, current drive, and divertor physics is the main research goal of NSTX. Substantial progress[3,4,5,6,7] was made in extending the operational regime of the device since the last IAEA conference, e.g. the achievement of discharges with β_t ~ 34%, β_N ~ 6.5, and pulse lengths ~ 1 sec. Routine access to H-mode operation has contributed to these operational regime advances. First, the β limit has been shown to increase[7] as the pressure peaking factor is reduced in NSTX, and H-modes lead to the lowest thermal pressure peaking factors ~ 2, due mainly to the broadness of the density profile. In comparison, the best L-mode discharge had a thermal pressure peaking factor ~ 2.6 and a β_N limit ~ 5. Second, the steep edge pressure gradient in H-modes has lead to high bootstrap fractions up to 40% and low loop voltage, enabling long pulse discharges. This paper describes the development of NBI-heated H-mode operation and H-mode physics research in NSTX; H-mode confinement relative to scalings and H-modes triggered by RF heating are discussed in a separate paper[8].

H-modes have been obtained[9] quite routinely in a broad parameter range in 2002: $0.6 \leq I_p \leq 1.2$ MA, $0.3 \leq B_t \leq 0.6$ T, $P_{NBI} \geq 0.32$ MW, $1.5 \times 10^{19} \leq \overline{n_e} \leq 6.5 \times 10^{19}$ m^{-3}, and $0.2 \leq \overline{n_e}/n_{GW} \leq 0.85$, where $n_{GW}[10^{20}\ m^{-3}] = I_p[MA]/\pi a^2[m]$ is the Greenwald density[10]. The first observed H-mode phases[11,12] in late 2000 and 2001 lasted only up to 70 msec; improved machine conditioning[13] (full plasma-facing graphite tile bake-out to 350 ^{o}C), reduction of the edge intrinsic error field[5], and the development of gas injector fueling from the center stack, i.e. the high-field side (HFS), enabled discharge reproducibility and an extension of the duration to over 500 msec (e.g. see references [3,4]).

Both lower-single null divertor (typically δ_{lower}~ 0.4) and double-null divertor (typically δ_{lower}~ 0.8) configurations allow H-mode access, although we note that upper single-null has not been attempted since reproducible H-modes were obtained. To date, the single null H-modes have produced the longest pulse lengths whereas double-null H-modes have produced the highest β_t. The single nulls are either quiescent, have very small edge-localized modes (ELMs, with $\Delta W/W<<1\%$ - see Fig. 1), or in a narrow fueling window just above the locked mode limit, very large ones ($4\%<\Delta W/W<20\%$, where W is the plasma stored energy). In the first 2 cases, $\overline{n_e}$ rises monotonically through the discharge; in the third case, the ELMs cause large edge density loss which fills in rapidly after the ELM, and the $\overline{n_e}$ rises monotonically between the large ELMs. Previously we have reported[9,11,12] that the edge density builds rapidly after the L-H transition and forms 'ears'. The duration of the present H-modes is sufficient to determine

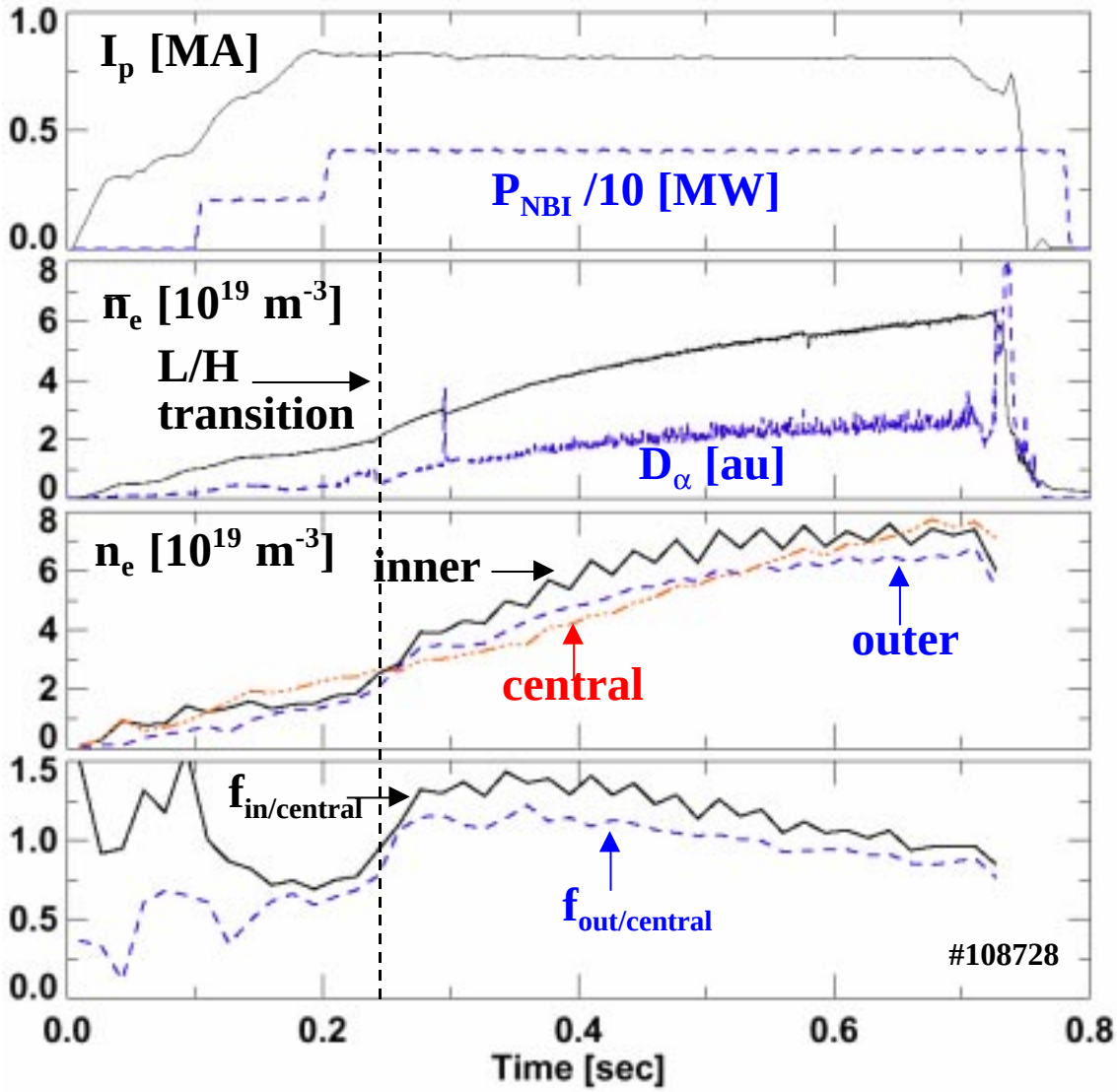

Fig. 1 – Time evolution of a long pulse H-mode. The inboard side H-mode pedestal density (R=46.7 cm), outer pedestal (R=142.0cm), and central n_e (R=100.7 cm) measured by Thomson Scattering are indicated in panel (c). The ratio of the inner pedestal to central density and outer pedestal to core density are shown in panel (d), showing that the core fills in more quickly than the edge. The point-to-point variability in $\overline{n}_e$ is due to laser-to-laser variation.

that the core density fills in faster than the edge density, leading eventually to a flat profile (Fig. 2). Double-nulls are characterized by discrete ELMs (either Type I or Type III, 1%<ΔW/W<4%) or are occasionally ELM-free, but somewhat surprisingly, the rate of density rise is nearly identical to single nulls.

The NBI heating power required for H-mode access has been measured[14] at two I_p values in lower-single null configuration with the ion Grad-B drift toward the X-point. At I_p=600 kA, P_{NBI}=320 kW ($P_{loss} \equiv P_{NBI}+P_{OH}$-dW/dT = 0.63 MW) was required to trigger an H-mode transition (B_t = 0.45 T, $\overline{n_e}$ =2.0 X 10^{19} m-3), and at I_p=900 kA, P_{NBI}=650 kW (P_{loss} = 1.2 MW) was required (B_t = 0.45 T, $\overline{n_e}$ =2.4 X 10^{19} m-3). Further experiments are required to determine if these data indicate an I_p dependence or a very strong $\overline{n_e}$ dependence, or a power threshold being reduced with wall conditioning. Both of the measured power threshold values are well above (~10-20 times) an early ITER scaling[15] based on conventional aspect ratio tokamaks. Recent inclusion of low aspect ratio data into the ITER database has yielded[16] an inverse aspect ratio dependence of the power threshold. A preliminary comparison with the new scaling indicates that the power threshold in NSTX is 3-4 times higher than the new scaling value.

One parameter clearly affecting H-mode access is the fueling characteristic near the NBI start time. Fueling from the HFS injector provides the most reliable H-mode access, as in the MAST device[17]. However the fueling rate can be either too low to allow H-mode access, resulting in a locked mode, or too high, resulting in a high loop voltage L-mode. Because of the long injector tube, the HFS gas injector has a large initial puff rate which decays in 10-15 msec followed by a slowly declining puff which continues for the discharge duration (see Fig. 3). A comparison of H-mode access and characteristics was made between discharges fueled by the HFS gas injector and an injector near the outer midplane (low toroidal field side, LFS) which was programmed for an identical flow rate. Fig. 3 shows that the discharge with the HFS gas injection had an H-mode transition about 75ms earlier than the LFS injection discharge, and also that the HFS injector fueled H-mode lasted longer. We note that the LFS fueled discharge had an L-H transition after the second NBI source was added at t=200 msec, indicating that the power threshold was higher for the LFS discharge. Fig. 4 shows that the toroidal rotation velocity (v_ϕ) and edge electron temperature were lower with LFS fueling, and that a bump in the outboard side electron density was present in the LFS fueled discharge just before the time of the L-H transition in the HFS fueled discharge. Variation of the timing of the programmed flow rate of the LFS injector failed to produce the same quality H-mode as the HFS injector fueled H-mode. As the gas injection rate was reduced, approaching the lower limit of H-mode access with HFS injection, the H-mode transition times and discharge characteristics became very similar between the two fueling locations.

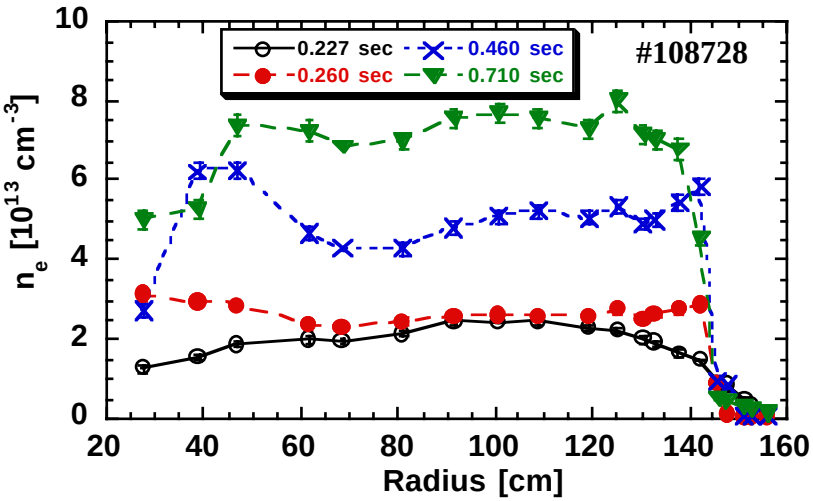

Fig. 2 – Evolution of density profile vs. time for the long-pulse H-mode in Fig. 1.

One additional note: H-mode access was also obtained by pre-loading the wall (in previous discharges) with high LFS gas puffing, and then cutting off external gas fueling at the onset of NBI. This technique was utilized[18] by the MAST team for H-mode access prior to their HFS fueling system. In NSTX, it produced comparable (but irreproducible) H-modes as compared

with HFS fueled H-modes, but with a presumably more distributed fueling source. Thus, it is clear that the poloidal location of the gas fueling has a measurable effect on H-mode access.

Investigation of the relationship between transport and turbulence in the H-mode edge is continuing with a gas puff imaging diagnostic[19,20] and a newly installed midplane reciprocating probe. The gas puff imaging diagnostic views a long, distributed gas puff source along the edge field lines. A narrow, quiescent emission band is observed in H-modes with small or no ELMs. The emission profile broadens and becomes much more turbulent in L-mode. The decrease in profile width in H-mode is consistent with a decrease in the emission region due to a decrease in the electron density gradient scale length. Detailed simulations with the DEGAS-2 atomic physics code, and the UEDGE and BOUT boundary transport codes are in progress. Data from a scrape-off layer reflectometer show[21] that the density gradient scale length itself fluctuates tremendously in L-mode, but is more quiescent in H-mode.

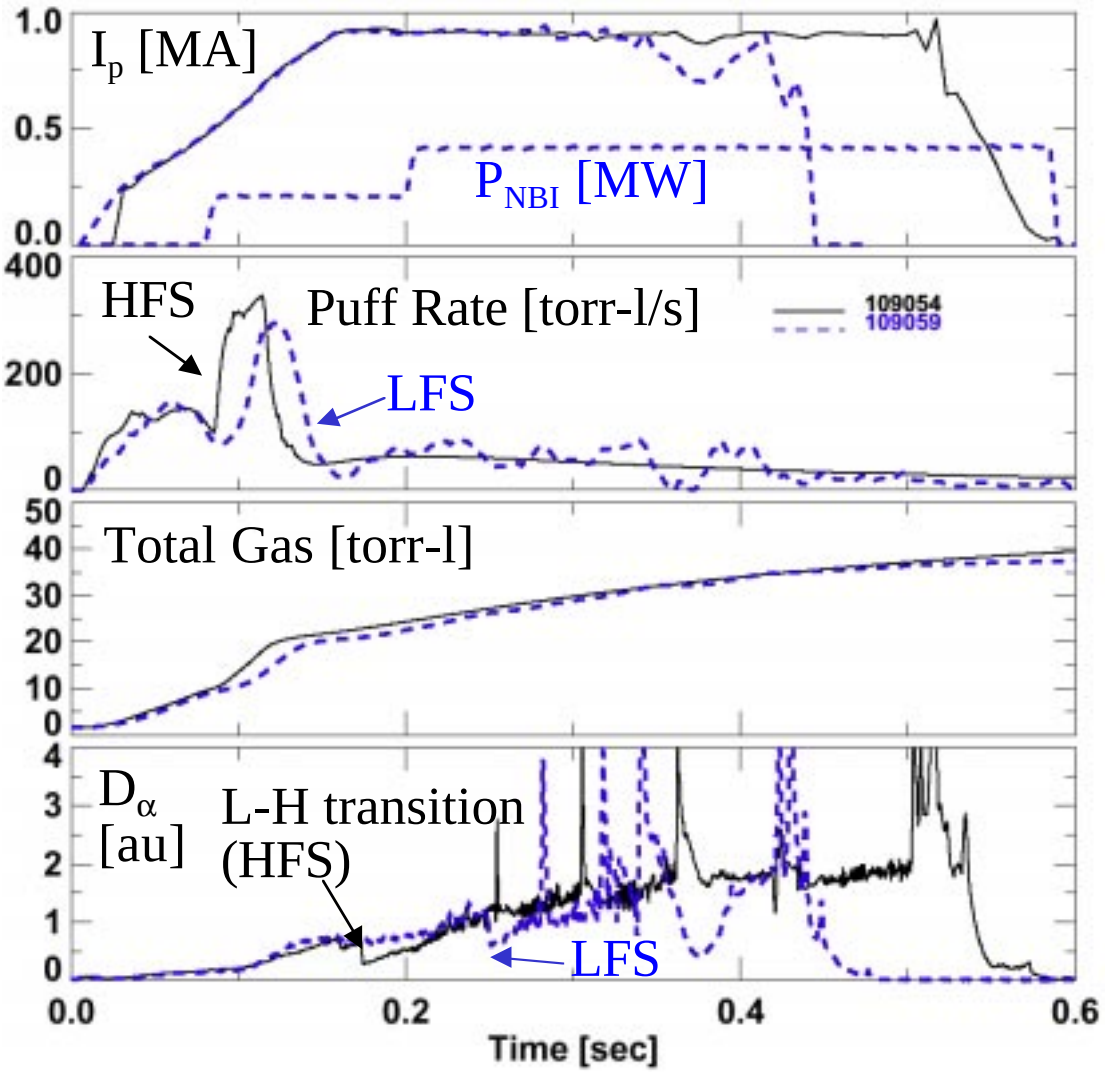

Fig. 3 – Comparison of a HFS and LFS fueled H-mode discharge. The NBI waveform displayed in panel (a) was used in both cases. The LFS injector was programmed to yield the same flow rate as the HFS injector. All gas fueling before t=90 msec. came from a second LFS injector and was not varied during this experiment.

The heat flux to the divertor targets has been measured in H-mode discharges. A quiescent lower-single null H-mode discharge was used (Fig. 5); approximately 3 times more power strikes the outer target than the inner target (Fig. 5c). This in/out power split is more balanced than the ≥ 9:1 split observed[22] in MAST double-null discharges. Power accountability is rather good: 70% of P_{loss} is observed at the target plates. In general, the core radiated power is about 10%, leaving about 20% for fast ion losses and divertor radiation. The peak heat flux in an L-mode with the same NBI power was about 33% higher, due to higher ohmic power and lower dW/dt; total power observed at the target plate as a fraction of edge power was also ~ 70%, i.e. comparable to the H-mode discharge. The profile width (full width at half maximum value) was slightly smaller in the H-mode (2.2 cm) than in the L-mode (~2.5 cm), but the H-mode width is at the limit of the instrumental resolution. Finally peak heat flux increased non-linearly with NBI power, up to a maximum value of 10 MW/m^2. The highest value observed[23] in L-modes was ~ 6 MW/m^2. A detailed scaling of the peak heat flux with input power and density will be obtained in coming experiments. Simulations of the heat flux and other edge data with the UEDGE code are in progress.

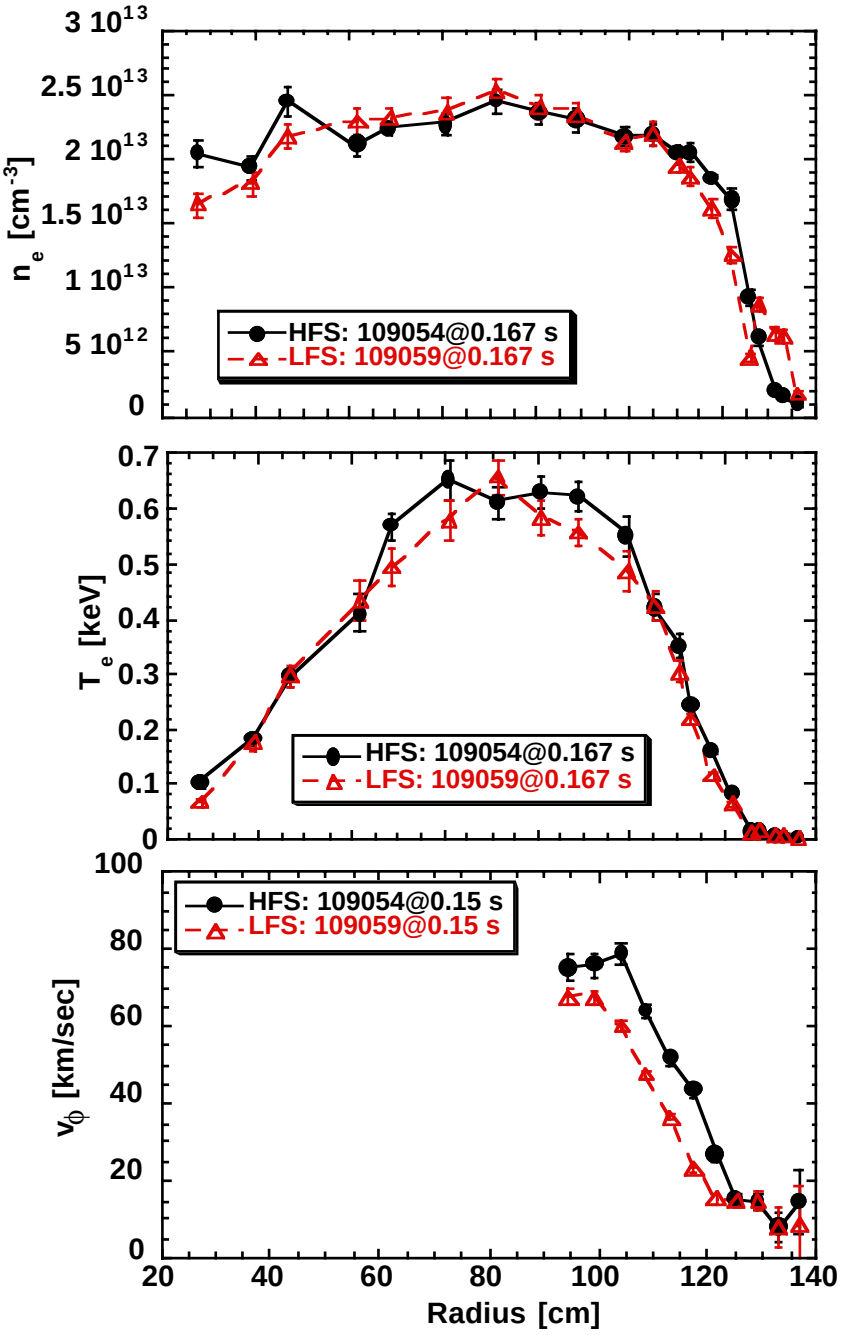

Fig. 4 – Comparison of n_e, T_e and v_ϕ profiles from the LFS fueled and HFS fueled discharges, The profile time for n_e and T_e is just before the HFS-fueled discharge L-H transition time, and the v_ϕ time is the closest available to the transition. Note the reduced edge T_e and n_e bump in the LFS fueled discharge, as well as the reduced velocity over the entire profile.

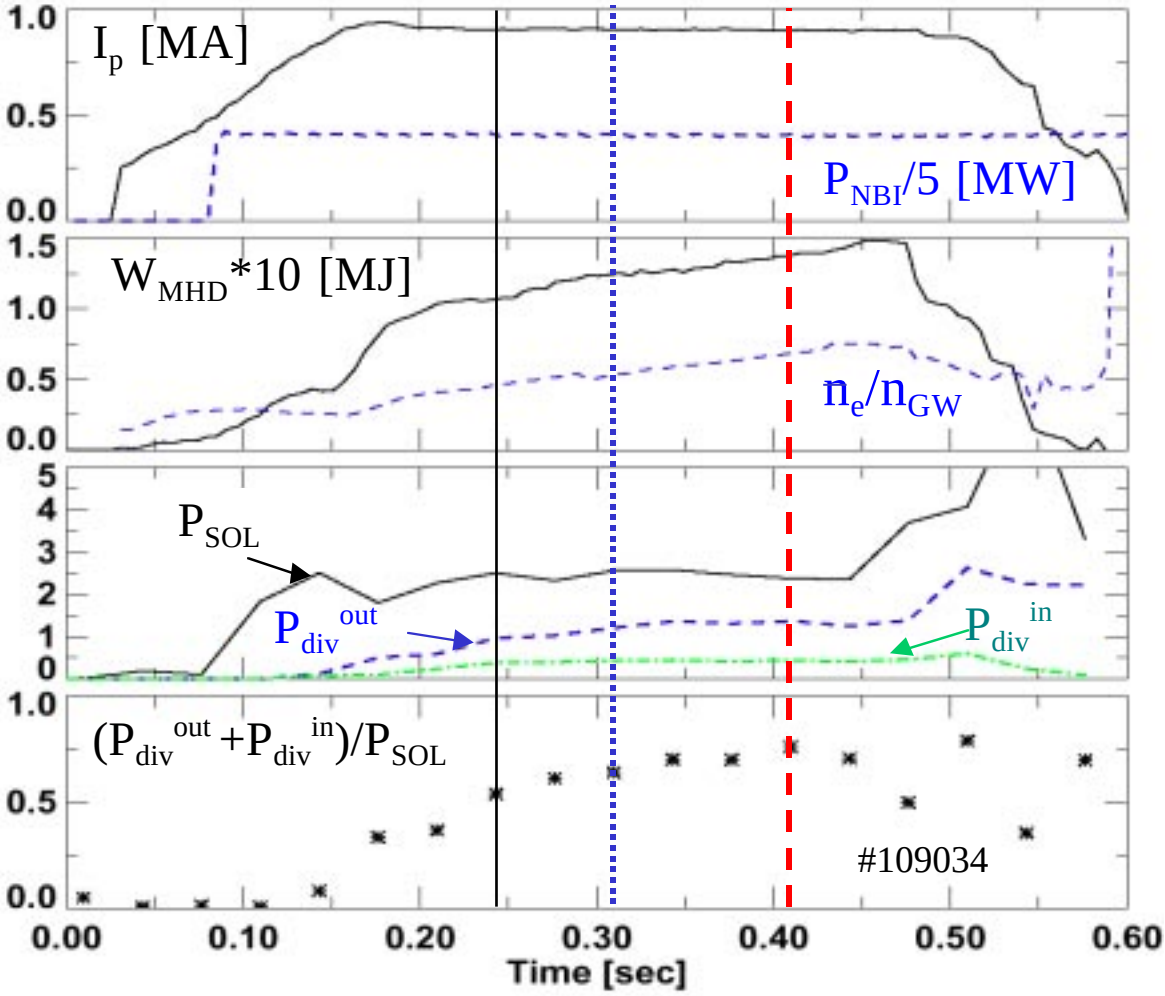

Fig. 5 – Time characteristics of the discharge used to assess divertor heat flux: (a) plasma current and NBI power, (b) plasma stored energy and density relative to Greenwald scaling, (c) total edge power (P_{SOL}), power to the inboard and outboard divertors (P_{div}^{in}, P_{div}^{out}), and (d) divertor power fraction. The L-H transition occurred at t=160msec, near the time of I_p roll-over. The dashed lines indicate profile times in Fig. 4.

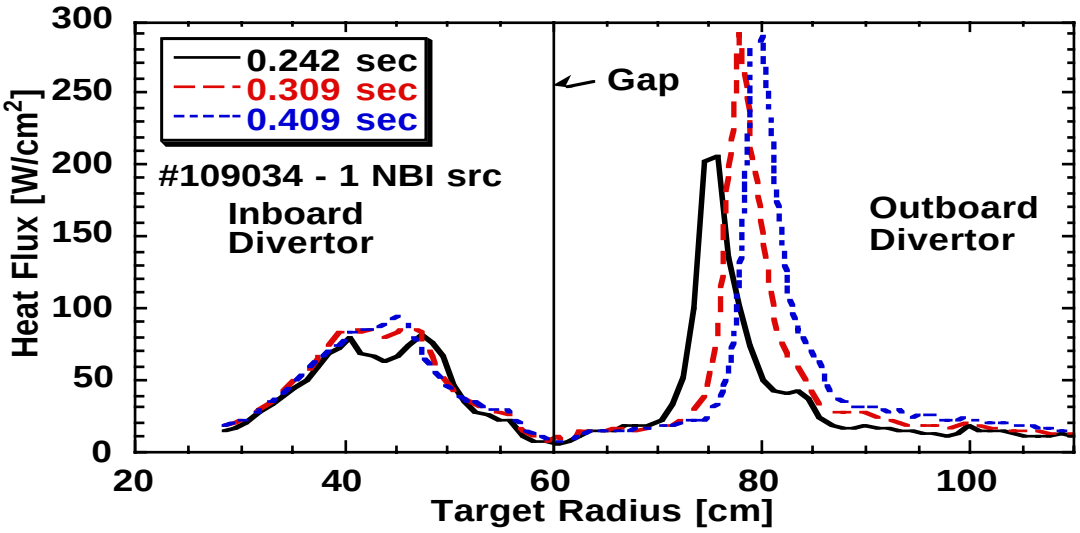

Fig. 6 – Divertor heat flux profile at several different times of discharge in Fig. 3. Note that the outer target profile shape comes to equilibrium after ~ 100ms on NBI injection, and the profile shifts to larger major radius during a natural strike point sweep.

In conclusion, H-mode operation has provided an operational scenario to further progress toward NSTX performance targets. Further optimization of the H-modes will include the use of improved fueling and heating control to create even broader pressure profiles for higher β limits. A divertor cryopump and advanced wall conditioning techniques are being considered for improved density control during discharges. In addition, research will continue on the physics of the termination of the H-mode phase after ~ 500msec. H-mode research in the past few years has focused on development as an operational tool, but an increasing emphasis is being placed on H-mode physics, in terms of access criteria (e.g. power threshold and fueling effects) and edge turbulence studies.

This research was supported by the U. S. Dept. of Energy under contracts DE-AC05-00OR22725, DE-AC02-76CH03073, DE-AC04-94AL85000, W-7405-ENG-36, W-7405-ENG-48 and grants DE-FG02-99ER54524 and DE-FG02-99ER54523. We gratefully acknowledge the contribution of the NSTX technical staff and neutral beam operations staff.

References

[1] Ono, M. et. al., *Phys. Plasmas* **4** (1997) 799.

[2] Neumeyer, C. et. al., *Fusion Eng. and Design* **54** (2001) 275.

[3] Maingi, R. et. al., "Recent Results from the National Spherical Torus Experiment", *Plasma Phys. Contr. Fusion* in press.

[4] Synakowski, E.J. et. al., this conference.

[5] Menard, J.E. et. al., this conference.

[6] Mueller, D. et. al., Proc. 29th International Conference on Plasma Science, Alberta, CA, June 17-22, 2002 in press.

[7] Sabbagh, S.A. et. al., this conference.

[8] LeBlanc, B.P. et. al., this conference.

[9] Bush, C.E. et. al., Proc. of 29th Euro. Conf. on Plasma Phys. and Contr. Fusion, Montreaux, SZ, June 17-22, 2002.

[10] Greenwald, M. et. al., *Nucl. Fusion* **28** (1988) 2199.

[11] Maingi, R. et. al., *Phys. Rev. Letts*. **88** (21 Jan. 2002) 035003.

[12] Bush, C.E. et. al., *Plasma Phys. Contr. Fusion* **44** (2002) A323.

[13] Kugel, H.W. et. al., "Impact of Wall Conditioning Program on Plasma Performance in NSTX", *J. Nucl. Mater*. in press.

[14] Bush, C.E. et. al., to be submitted to *Phys. Plasma*, 11/02.

[15] Snipes, J.A. et. al., Proc. 24th Euro. Conf. on Plasma Physics and Contr. Fusion, Berchtesgaden, Germany (1997: Geneva), part III, p. 961.

[16] Valovic, M., presented at the ITPA Confinement, Database, and Modeling Working Group Meeting, Princeton, NJ, March 8-11, 2002.

[17] Field, A.R. et. al. *Plasma Phys. Contr. Fusion* **44** (2002) A113.

[18] Sykes, A. private communication, 2001.

[19] Zweben, S.J. et. al., *Phys. Plasma* **9** (2002) 1981.

[20] Maqueda, R. et. al., Proc. 14th High Temp. Plasma Diagnostics Conf., Madison, WI, 8-11 July, 2002.

[21] Wilgen, J.G. private communication, 10/2002.

[22] Counsell, G.W. et. al. "A Review of Plasma Boundary Phenomena in the Mega Amp Spherical Tokamak", *J. Nucl. Mater*. in press.

[23] Maingi, R. et. al., "Heat Flux Scaling Results in NSTX", *J. Nucl. Mater*. in press.